RETRODIRECTIVE ROTMAN LENS ANTENNA

S Christie [(1)], R Cahill [(1)], N Buchanan [(1)], V Fusco [(1)],
N Mitchell [(1)], Y Munro [(2)], G Maxwell-Cox [(2)]

[(1)] *The Institute of Electronics, Communications and Information Technology (ECIT), Queen's University Belfast, Northern Ireland Science Park, Queen's Road, Queen's Island, Belfast BT3 9DT, Northern Ireland, UK, Email:r.cahill@ecit.qub.ac.uk*

[(2)] *EADS Astrium, Earth Observation & Navigation Directorate, Anchorage Road, Portsmouth PO3 5PU, Hampshire, UK*

ABSTRACT

The purpose of this paper is to present the theoretical design of a passive retrodirective array architecture based on a microstrip Rotman lens. The true time delay property of the beamforming network is exploited to perform automatic high gain antenna pointing with broadband capability. The analysis and performance optimisation is carried out using Remcom Rotman Lens Designer (RLD) software and CST Microwave Studio (MWS) and requires design features not normally considered when the lens is operated as a beamforming network for an array. The structure, which has 21 beam and 12 array ports, is designed to minimise bistatic beam pattern squinting and monostatic RCS ripple over the frequency range 8 – 12 GHz.

1. INTRODUCTION

A retrodirective array has the property of automatically re-transmitting a received signal toward its source with no prior knowledge of the source location. This gives it the ability to automatically track rapidly moving signal sources, reduce interference and improve the signal to noise ratio in a satellite or mobile communications link. Retrodirective arrays have no requirement for motors, phase shifters or power hungry DSP, and therefore for some applications these offer an attractive alternative to phased and adaptive arrays, and mechanically scanned antennas. As such, they have been proposed for a number of space and terrestrial applications, including high gain satellite communications links [1], power transmission from solar powered satellites [2] [3], radar [4], radar cross section (RCS) enhancement [5] and spatial division multiple access for mobile communications [6].

Two well known retrodirective architectures are the Van Atta array [7] and the heterodyne retrodirective array [8]. In the Van Atta array, Figure 1a, symmetrically located elements are connected through a series of equal length delay lines. When a wavefront is incident on the Van Atta a phase lag is produced across the array, which is dependent upon the Angle of Incidence (AOI). The delay lines effectively turn the phase lag in the received signal into a phase lead in the re-transmitted signal, directing the re-transmitted wavefront towards the source of the incoming signal. The Van Atta described is passive and has a wide bandwidth provided TEM lines and wideband antennas are used. The lines increase in length and complexity as the size of the array is increased and this also reduces the antenna efficiency. Active variants are available but require components such as amplifiers and either mixers and local oscillators or circulators [6].

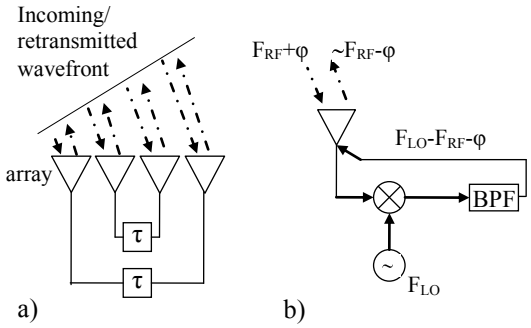

Figure 1. a) Van Atta architecture; b) Single element of a heterodyne retrodirective array

The heterodyne retrodirective array, Figure 1b, performs phase conjugation at each array element by mixing the signal with a local oscillator at approximately twice its frequency, and filtering unwanted products. The heterodyne architecture allows modulation of the retransmitted signal, but it is inherently narrow band, and the performance is degraded by beam squinting as frequency is varied from the centre operating frequency. Moreover, the use of active components increases the cost of the antenna, and the mixer conversion loss can often be prohibitively high.

This paper describes a new passive retrodirective array architecture which was implemented using a broadband

Rotman lens. The reciprocity property of the beam forming network is exploited to produce a single lens based retrodirective array antenna by terminating the input ports of the structure with open circuits. The received signal from the in-focus beam port is automatically re-transmitted towards its source, with the optical path lengths in the lens providing the required phase conjugation. Inherent in this simple low profile design is a true time delay phase shift capability which provides frequency independent self tracking. The principle of operation is demonstrated by employing two numerical simulators to optimise the geometry and simulate the bistatic and monostatic RCS of a Rotman lens which gives a scan coverage of ±40° and operates over the frequency range 8 – 12 GHz.

2. THE ROTMAN LENS

2.1. Principle of Operation

The Rotman lens, Figure 2, was first presented in [9]. It is a microwave beam-former which feeds a linear array of antennas, and features N input (beam) ports connected to M output (array) ports, through a parallel plate lens cavity and a section of 'correction' transmission lines. The lens is most commonly fabricated using waveguide or microstrip technologies.

The beamforming operation of a conventional Rotman lens is imposed by a set of design equations presented in [9], which specify the geometry of the lens beam and array contours and the relative correction line lengths for a given scan coverage. In transmit mode a beam port is excited with a signal which spreads through the lens cavity and is received by the antenna elements. Steered beams are formed as a result of the optical path lengths from the beam port to the transmitted wavefront, as illustrated by Figure 2a. The lens is a True Time Delay (TTD) device because the beam-steering mechanism is dependent upon these propagation path lengths, rather than a phase slope across the array. This property provides an inherently wide bandwidth, which is in practice limited only by the radiating elements or dispersion in the transmission line medium.

Exciting the lens at its three focal points F_1, G and F_2 forms beams at $\alpha°$, 0° and $-\alpha°$ to the array respectively, where α is a specified design variable, and is also the angle between each of the outer focal points and the centre of the array contour.

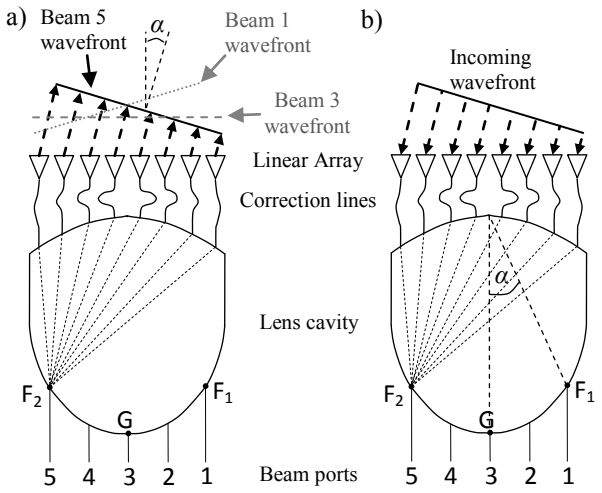

Figure 2. Rotman Lens Operation; a) transmit; b) receive

Exciting the beam ports situated between the focal points forms beams between 0° and ±α°, with the n^{th} beam port forming a beam at;

$$\theta° = \alpha° \left(\frac{N-2n+1}{N-1}\right) \quad (1)$$

An ideal lossless lens is reciprocal, as illustrated by Figure 2. In receive mode an incoming wavefront arrives with a time lag across the linear array. As a result, the signals sampled by each element travel through the correction lines and lens cavity, and add in phase mainly at one (or two) of the beam ports. The beam port(s) upon which the signal is focused is dependent upon the incoming wavefront's AOI, which allows passive detection of the direction of the signal source.

2.2. Retrodirective Rotman Lens

Retrodirective arrays using multiple Rotman lenses have previously been applied for high power radar jamming applications [10]. The lens presented here is a novel passive single lens implementation which is based on similar principles. To achieve retrodirectivity, the lens beam ports are all open-circuited. When a wavefront is incident on the array at θ° it focuses mainly on one (or two) of the beam ports, as illustrated in Figure 2b. The open-circuit reflects the focused signal, setting up a transmitted wavefront at θ° to the boresight direction of the array due to the lens's reciprocity.

The retrodirective Rotman lens offers several potential advantages over other retrodirective architectures. It has an inherently wide bandwidth due to its TTD behaviour, and is cheap and simple to fabricate. There is no increase in complexity as the number of radiating elements in the array is increased (as is the case with the

Van Atta array), and there is no need for components such as mixers and filters which increase cost and narrow the bandwidth of the heterodyne arrangements. The lens based architecture also offers several useful features not readily available in other retrodirective arrays. These include; the ability to passively detect the AOI by comparing the signal amplitude at each beam port; the ability to selectively block signals from certain AOIs by proper termination of corresponding beam ports to absorb rather than reflect focused signals; and the potential to passively phase modulate the back scattered signal by switching between open and short-circuit terminations. Alternatively, the terminations could be replaced with MMIC reflection amplifiers, offering an increase in gain and the potential to amplitude modulate back scatter, using the approach discussed in [11].

3. DESIGN PROCEDURE

3.1. Numerical simulators

Remcom Rotman Lens Designer (RLD) software [12] was used for parametric studies and the initial theoretical design of the beamformer in transmit mode. This fast design tool is based on Geometric Optics (GO) and approximates the coupling between an i^{th} beam port, and a j^{th} array port, using equation 2 [13].

$$S_{ij} = \frac{\sin(x_i)}{x_i}\frac{\sin(x_j)}{x_j}\sqrt{\frac{w_i w_j}{\lambda r}}e^{-j(kr+\frac{\pi}{4})} \quad (2)$$

where w_i is the width of port i, φ_i is the angle between the normal to port i and the direction of port j, and $x_i=kw_i\sin(\varphi_i)/2$.

RLD gives the complex excitation co-efficients across the array ports when one or more beam ports are excited, but this model does not take account of reflections from the lens sidewalls, and mutual coupling between the lens correction lines, which cause phase and amplitude errors. For more accurate predictions, the lens designs were exported from RLD into the Transient Solver in CST MWS to carry out a rigorous 3D EM analysis. The CST simulation S-parameter results give the complex excitation co-efficients (A_n) across the lens's array ports. For both numerical models equation [14] was used to generate the Array Factor Gain (AFG) (assumes no mutual coupling between the omnidirectional antennas) and equation 4 [15] was employed to predict the Insertion Loss (IL).

$$AFG\ (dB) = 20log_{10}\left(\sum_{n=1}^{N} A_n\, e^{j2\pi(n-1)u}\right) \quad (3)$$

where $u=d/\lambda(\sin\theta-\sin\theta_0)$.

$$IL\ (dB) = 10log_{10}\sum_{n=1}^{N}|A_n|^2 \quad (4)$$

In the CST model the beam ports of the retrodirective Rotman lens were open circuited and to simulate an incoming wavefront the array ports were simultaneously excited with equal amplitude signals. A progressive time delay between consecutive array ports was used to model the performance of the array for signals incident at angles off boresight. This was varied according to;

$$TIME\ DELAY\ (s) = \frac{dsin(\theta)}{3x10^8} \quad (5)$$

where d is the element spacing, and $\theta°$ is the AOI. The far field radiation patterns were generated by inserting the predicted scattering parameters into equation 3.

In addition to providing more accurate simulation results, CST MWS allows the fields within the lens to be viewed. Figure 3 shows surface current plots at 10 GHz in transmit and receive mode for a microstrip lens constructed on a 0.64 mm thick Taconic RF-60A substrate with ε_r=6.15. The lens has 9 array ports and 7 beam ports, and was designed to give a scan coverage of α=30°.

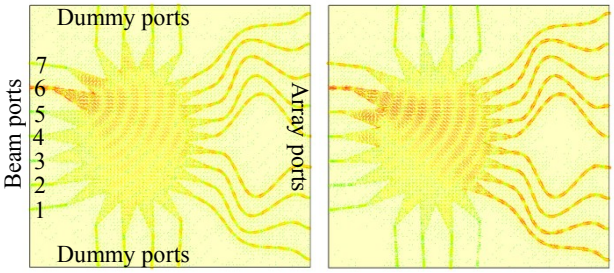

Figure 3. Surface current in a 9-element lens design; a) with beam port 6 excited; b) with wavefront arriving at 20° to array and focusing on beam port 6

The ability to investigate the lens in this way allows a useful insight into its behaviour in terms of identifying sources of loss and causes of performance degradation. For example the lens sidewalls are lined with 'dummy ports', which are terminated with matched loads to absorb incident energy and minimise interference across the array due to reflections. Surface current plots provide an illustration of the mechanism of power loss due to 'spillover' onto these dummy ports. Comparing surface current plots of the lens in transmit and receive mode shows that the lens is not perfectly reciprocal. This can be seen in Figure 3, where the spillover in transmit mode is predominantly onto the lens sidewalls and therefore is mainly absorbed, whereas in receive mode it is predominantly onto the ports adjacent to the in-focus beam port. This reduces insertion loss in the retrodirective lens, as the spilled over signals are also reflected and retransmitted. For the latter case the array

port excitation is uniform (corresponding to plane wave excitation of the array) whereas for the former operating mode an amplitude taper is created across the aperture.

3.2. Design Considerations

Exciting the Rotman lens at one of its beam ports forms either a boresight directed or a tilted primary beam, as discussed in section 2.1. Simultaneously exciting two adjacent beam ports with the correct phasing forms an intermediate beam between the two primary beams. This is an important consideration for the retrodirective lens design, because the AOI may be such that the incoming signal is simultaneously focused onto two beam ports. It is essential therefore that in this case the signals are reflected from the two in-focus beam ports in such a way that they give rise to an intermediate beam which is pointed towards the signal source. Performance optimisation of the retrodirective lens must include several additional design steps which are not normally considered when the lens is operated as a beamforming network for an array.

3.2.1 Beam port excitation phase

The phasing necessary to form intermediate beams was investigated in transmit mode in CST MWS for the lens shown in Figure 3. Figure 4 shows the array factors which result from simultaneously exciting adjacent beam port pairs 4 and 5, 5 and 6, and 6 and 7.

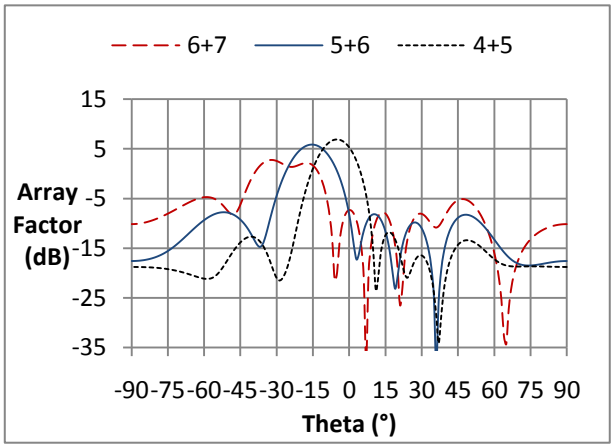

Figure 4. Intermediate beams due to simultaneous excitation at 10 GHz

Simultaneously exciting ports 4 and 5 forms a beam with a gain of 6.8 dB at -5°, which is directly between the primary beams generated by excited port 4 (0°) and port 5 (-10°). Simultaneously exciting ports 5 and 6 produces a beam at -15°, again midway between the two primary beams, but in this case the gain is 1 dB lower than the intermediate beam at -5°. The beam formed by exciting ports 6 and 7 should have a peak at 25°, but Figure 4 shows that the pattern is distorted and a peak null occurs at this angle.

Investigation of the surface current shows that this distortion is due to the unequal propagation lengths from ports 6 and 7 to array ports. This creates an interference pattern within the lens, and the asymmetric aperture distribution exhibits a null at the centre of the array port contour, as shown in Figure 5a. In order to correct this, the approximate time taken for a signal to propagate from each of the beam ports to the centre of the array port aperture is calculated. This is used to correct the port excitation phase such that signals from ports 6 and 7 arrive simultaneously thus giving rise to constructive interference, with energy better focused on the centre of the contour, as shown in Figure 5b. Therefore for high performance retrodirective operation the Rotman lens design must consider the length of the individual 50Ω transmission lines at the beam ports.

a) b)

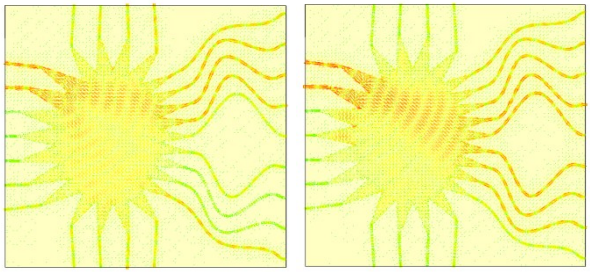

Figure 5. Surface current plots with; a) beam ports 6 and 7 simultaneously excited; b) beam ports 6 and 7 excited with time shift

3.2.2 Aperture size

Correct phasing of the adjacent beam port pairs creates well formed intermediate beams which have similar levels of gain. The intermediate beams are broader than the primary beams, but in the case of the 9-element design, they have higher gains, typically 0.75 – 1.5 dB, as shown in Figure 6. This is because exciting two ports with the necessary phasing reduces spillover loss onto the dummy ports by focusing energy onto the centre of the array port contour, as can be seen by comparing Figures 3a and 5b. For the same reason the directivity of the intermediate beams is reduced because of the increase in amplitude taper across the array ports.

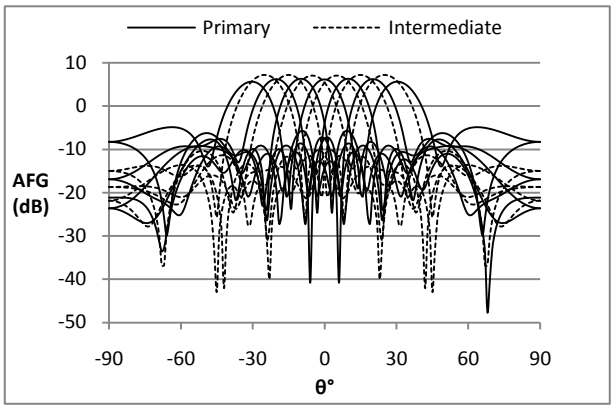

Figure 6. Primary and intermediate beams for 9-element lens design at 10 GHz

However, for larger arrays this is not always the case. For example, the simulated plots depicted in Figure 7 show that a Rotman lens with 14 array ports and 7 beam ports generates primary beams which have higher gains (typically 1.2 – 2 dB) than the intermediate beams. Increasing the number of array elements from 9 to 14 increases the directivity of the primary beams, as well as reducing spillover loss due to a larger array port aperture. The intermediate beams (generated by exciting two beam ports simultaneously) formed by the 14 element lens have lower spillover loss than the primary beams, but this reduction is much less significant than for the 9-element lens, and is not large enough to offset the higher directivity of the primary beams.

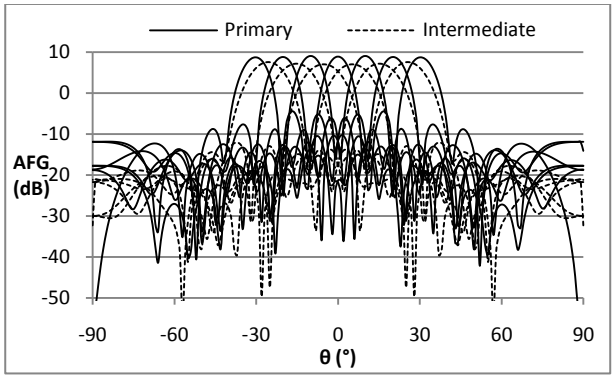

Figure 7. Primary and intermediate beams for 14-element lens at 10 GHz

These results indicate the importance of correctly choosing the number of array elements in order to reduce the monostatic RCS ripple when the Rotman lens is employed as a retrodirective array antenna.

4. RETRODIRECTIVE LENS DESIGN

A retrodirective lens is designed for operation from 8 – 12 GHz with a field of view of ±40°. The substrate used is 0.64 mm thick Taconic RF-60A with ε_r=6.15 and $tan\delta$=0.0038. The geometry of the optimised design is shown in Figure 8.

A number of important considerations were taken into account during the design process. The array port spacing is set at 0.5λ at 12 GHz to prevent grating lobes, according to equation 6 [16];

$$d \geq \frac{\lambda}{1+sin\theta} \tag{6}$$

The method discussed in section 3.2.1 of phasing adjacent beam ports to form intermediate beams is implemented by varying the relative lengths of the beam port to open circuit microstrip lines. This ensures that when a received signal is focused onto two adjacent beam ports the reflections from each port arrive in phase at the centre of the array, producing a transmitted intermediate beam which is pointed in the desired direction.

The numbers of beam and array ports are chosen to minimise the monostatic RCS ripple which was discussed in section 3.2.2. Using 12 array ports gives primary and intermediate beams which have similar gains and using 21 beam ports gives a reasonably high resolution, with a tilt angle of 5° between primary beams, and 2.5° between intermediate beams.

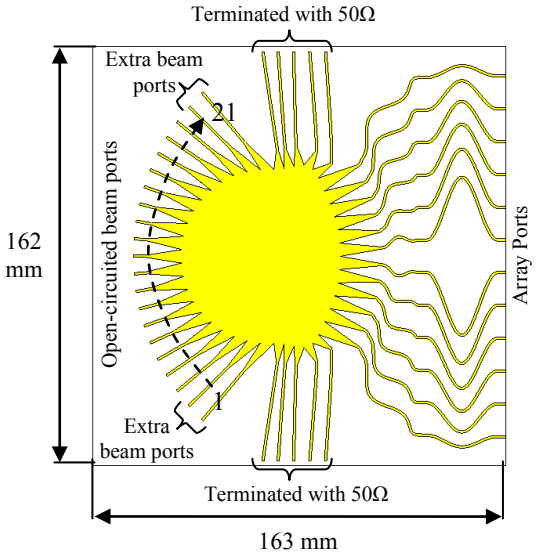

Figure 8. Retrodirective Rotman Lens Design

For this retrodirective design we have minimised the beam squint angle by considering the energy coupled to the individual beam ports. The incoming signal is never perfectly focused onto the one (or two) desired beam port(s). Spillover energy is reflected together with the primary reflection, and the resulting interference can cause beam tilt. Figure 9 shows the coupled power to each of the retrodirective lens's beam ports at 10 GHz when signals arrive at AOIs of 0°, 20° and 40°.

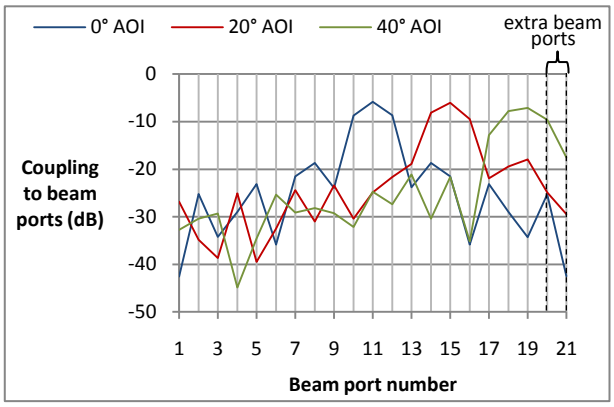

Figure 9. Focusing of signal onto lens beam ports in receive mode for different AOI at 10 GHz

When the AOI is at 0° to the array boresight direction, 31% of the signal power is focused primarily onto beam port 11, with symmetrical spillover of 15% onto each of beam ports 10 and 12. Less than 1.3% of power is spilled onto each of the other beam ports. As such, the reflection of the symmetrical power spillover effectively reinforces the desired reradiated beam, and predicted beam squint is negligible. For an AOI of 20°, 25% of the signal power is focused onto beam port 15, with 15% and 11% spilled onto ports 14 and 16 respectively. Spillover onto each of the other beam ports is less than 1.6 %. The asymmetrical excitation of the adjacent ports causes the reradiated beam to squint through an angle <0.3°. For an AOI of 40°, there is more significant spillover onto the four adjacent beam ports, rather than two in previous examples. For this case, ports 3 and 19 generate primary beams in the directions α=±40°, and 19% of the signal power is focused onto port 19 (3), with 5%, 16%, 11% and 2% focused onto ports 17 (5), 18 (4), 20 (2) and 21 (1) respectively. The addition of the extra ports 1, 2, 20 and 21 is necessary to improve the illumination symmetry and the computed results show that this design feature reduces tilt angle to <0.3° at 10 GHz.

The predicted bistatic RCS patterns of the retrodirective Rotman lens are shown in Figures 10, 11 and 12 with the source positioned at 0°, ±10°, ±20°, ±30° and ±40°. For each incident angle the patterns are predicted at frequencies of 8 GHz, 10 GHz and 12 GHz. When the bistatic patterns are examined at 2.5° increments within the ±40° range, the worst case beam squinting reduces as frequency increases, from 0.6° at 8 GHz, to 0.3° at 10 GHz, and 0.2° at 12 GHz. The efficiency of the lens is between 42.6% – 47.9 % at 8 GHz, 33.5 – 38 % at 10 GHz, and 31 – 34.3 % at 12 GHz. The individual sources of loss in the lens are summarised in Table 1 for retrodirective operation for a boresight directed wavefront. For comparison, Table 2 shows the sources of loss for transmit mode, with a single beam port excited and all others terminated with matched loads.

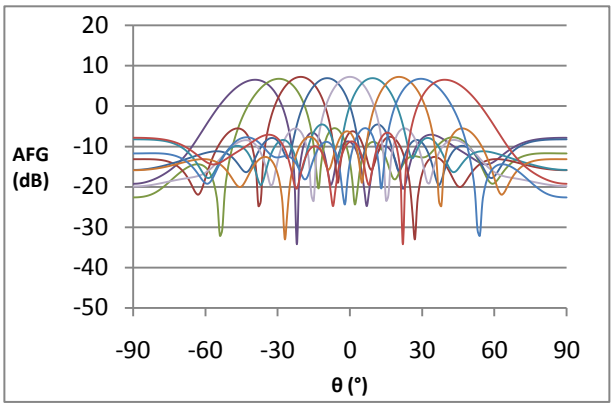

Figure 10. Predicted Bistatic Array Factors at 8 GHz

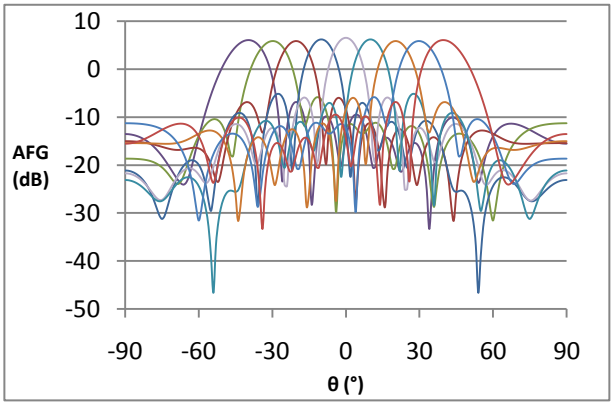

Figure 11. Predicted Bistatic Array Factors at 10 GHz

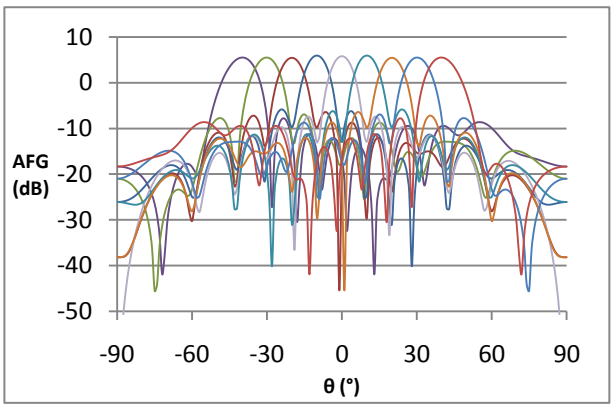

Figure 12. Predicted Bistatic Array Factors at 12 GHz

Table 1. Sources of loss in retrodirective lens with a boresight directed wavefront

	% of Input Signal Power Loss		
Source of Loss	8 GHz	10 GHz	12 GHz
Ohmic	8.2	9.3	10.6
Dielectric	29.4	36.9	41.6
Spillover	6.3	2.3	0.55
Radiation	9.2	13.9	16.5

Table 2. Sources of loss in transmit mode with a boresight directed wavefront

	% of Input Signal Power Loss		
Source of Loss	8 GHz	10 GHz	12 GHz
Ohmic	2.1	2.6	3
Dielectric	6.4	9.2	12
Spillover	56.3	49.8	50.9
Radiation	2.3	4.2	3.7
Return loss	8.2	7.6	2.2

The lens efficiency is improved in retrodirective operation compared to transmit mode. This is largely due to a reduction in spillover, from a worst case of 56.3% in conventional transmit mode to a worst case of 6.3% in retrodirective operation. The reason for this is that in retrodirective mode the power which is incident on the beam port contour is all reflected, giving a larger effective beam port aperture, and hence better focusing of energy onto the array ports, as depicted in Figure 13. Ohmic and dielectric losses become a more severe source of loss for retrodirective operation due to a doubling of the propagation path lengths within the lens. It is possible to reduce these losses through choice of the technology used to fabricate the lens, and most notably, a low loss dielectric could significantly improve the efficiency of the microstrip retrodirective Rotman lens. It is important to note that the spillover, return and radiation losses are calculated for a lens with no dielectric or conductive losses, in order to fully account for the power loss within the lens. In practice with these accounted for between 6.9% to 10.8% of the input power is radiated, and power coupled to the dummy ports is reduced. Return loss is not considered for the retrodirective lens as all energy reflected towards the array ports effectively reduces the insertion loss.

a) b)

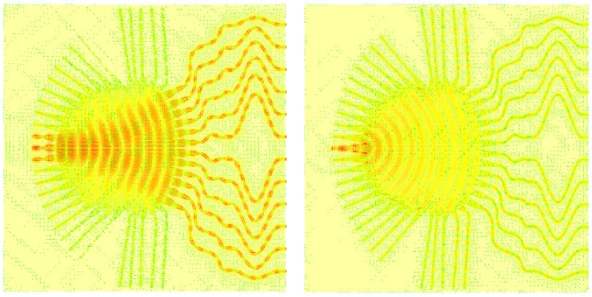

Figure 13. Lens surface current at 10 GHz with a boresight directed wavefront in a) retrodirective operation, b) transmit mode

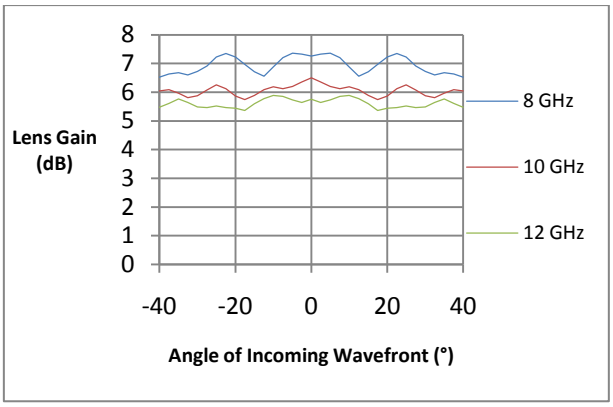

Figure 14. Predicted Monostatic RCS Ripple

The predicted monostatic RCS depicted in Figure 14 demonstrates that the source point is always tracked by the peak of the radiation pattern. The monostatic ripple, computed in the scan range of ±40° and increments of 2.5° is shown to decrease with frequency, with a maximum ripple of 0.83 dB at 8 GHz, 0.63 dB at 10 GHz, and 0.45 dB at 12 GHz.

5. CONCLUSIONS

The theoretical design and analysis of a retrodirective antenna architecture based on the Rotman lens has been presented. Important design considerations have been outlined, and methods to minimise beam squinting and monostatic RCS ripple have been applied. A technology demonstrator operating over a 40% bandwidth centred at 10GHz is shown to give a maximum beam squint angle of 0.6° and 0.83 dB gain ripple over ±40°. The lens efficiency was found to vary between 31% and 47.9% over the 8 – 12 GHz frequency band which is comparable to conventional microstrip Rotman lenses operating in transmit or receive mode only [17], [18]. For applications at higher frequencies waveguide can be applied to minimise losses in the lens [15]. The results of this study demonstrate that the Rotman lens can perform beam steering and tracking very well. This offers a low cost array architecture with the ability to determine signal direction, selectively block signals, and provide signal amplification and modulation. However, further work is required to establish the effect of scan loss which occurs when non omnidirectional antennas are employed as radiating elements, and moreover the impact on performance when the electromagnetic coupling is not negligible. These simulated results and scattering parameter and RCS measurements will be presented at the workshop.

6. ACKNOWLEDGEMENTS

Steven Christie is supported by a CEOI (www.ceoi.ac.uk) sponsored NERC PhD studentship and an EADS Astrium CASE award.

7. REFERENCES

1. Hansen, R.C. (1964). Preface to the special issue on active and adaptive antennas. *IEEE Trans. Antennas Propaga.* **12**(2), 140-141

2. Brown, W.C. (1981). Status of the Microwave Power Transmission Components for the Solar Power Satellite (SPS). In *IEEE MTT-S International Microwave Symposium Digest*, pp 270-272.

3. McSpadden, J.O., Little, F.E., Duke, M.B., Ignatiev, A. (1996). An In-Space Wireless Energy Transmission Experiment. In *Proceedings of the 31st Intersociety Energy Conversion Engineering Conference*, **1**, pp. 468-473

4. Gupta, S., Brown, E.R. (2003). Retro-directive Noise Correlation Radar with Extremely Low Acquisition Time. In IEEE MTT-S Microwave Symposium Digest, **1**, pp. 559-602

5. Fusco, V.F., Toh, B.Y. (2002) Retrodirective Array Augmentation for Electronic *RCS* Modification. IEEE Trans. On Microwave Theory and Techniques. **50**(7), 1772-1778

6. Fusco, V.F., Karode, S.L. (1999). Self-phasing Antenna Array Techniques for Mobile Communications Applications. *Electron. and Comm. Eng. Journal.* **11**(6), 279-286

7. Van Atta, L.C. (1959). Electromagnetic Reflector. *US Patent 2W8002*

8. Pon, C.Y. (1964). Retrodirective Array Using the Heterodyne Technique. *IEEE Trans. Antennas Propaga.* **12**(2), 176-180

9. Rotman, W., Turner, R.F. (1963). Wide Angle Microwave Lens for Line Source Applications. *IEEE Trans. Antennas and Propaga.* **11**(6), 623-632

10. Archer, D.H., Maybell, M.J. (2005). Rotman Lens Development History at Raytheon Electronic Warfare Systems 1967-1995. In *Proc 2005 IEEE Antennas and Propaga. Soc. Int. Symposium,* **2B**, pp 31-34

11. Xue, L., Cantu, H.I., Fusco, V.F. (2007). Two-Dimensional Luneburg Lens RCS Augmentation Using MMIC Reflection Amplifier. In *Proc 3rd Loughborough Antennas and Propaga. Conference*, pp 81-84

12. Remcom's official webpage for the Rotman Lens Designer software. Online at *http://www.remcom.com/rotman-lens-designer* (as of 1 August 2010)

13. Maybell, M.J. (1981). Ray Structure Method for Coupling Coefficient Analysis of the Two Dimensional Rotman Lens. In *Proc. Antennas and Propaga. Soc. Int. Symposium*. **19**, pp. 144-147

14. Hansen, R.C. (1998). Linear Array Pattern Synthesis. In *Phased Array Antennas*, Wiley Interscience, pp. 47-105

15. Rausch, E.O., Peterson, A.F., Wiebach, W. (1997). Electronically Scanned Millimeter Wave Antenna Using a Rotman Lens. In *Proc. Radar 97 (Conf. Publ. No. 449),* pp 374-378

16. Hansen, R.C. (1998). Basic Array Characteristics. In *Phased Array Antennas*, Wiley Interscience, pp. 7-46

17. Schulwitz, L., Mortazawi, A. (2006). A New Low Loss Rotman Lens Design for Multibeam Phased Arrays. In *IEEE MTT-S International Microwave Symposium Digest.* 445-448

18. Cheng, Y.J., Hong, W., Wu. K. (2010). Design of a Substrate Integrated Waveguide Modified R-KR Lens for Millimeter-wave Application. *IET Microwaves, Antennas and Propaga.* **4**(4), 484-491